# Estimation With Range Dependent Sensor Model


Vahram Stepanyan *
*NASA Ames Research Center, KBR Wyle Services, Moffett Field, CA 94035*

Thomas Lombaerts†
*NASA Ames Research Center, KBR Wyle Services, Moffett Field, CA 94035*

Chester V. Dolph‡
*NASA Langley Research Center, Hampton, Virginia 23681*

Corey Ippolito §
*NASA Ames Research Center, Moffett Field, CA 94035*



**This paper focuses on the improvement of target tracking accuracy taking into account the sensor's reading degradation as the relative range increases. The approach is based on the assumption that range measurement error depends on the actual range. Specifically, we model the measurement error as a proportional to the actual range term plus a zero-mean, Gaussian distributed, and uncorrelated process. We present two approaches to tracking a target with constant velocity model. The first approach uses Extended Kalman Filter (EKF) framework to estimate target's states and the unknown proportionality coefficient with linearization on the observation model on the predicted states at each time step. The second one uses a measurement conversion method to estimate the target's scaled by the unknown constant term states, which is shown to be unbiased. This conversion results in linear state and observation models, hence the standard Kalman filter can be applied. The actual target state is computed by application of back scaling with the estimate of unknown scale factor. We evaluate the approaches in desktop simulations.**


## I. Introduction

Advanced Air Mobility (AAM) is a revolutionary air transportation system for passengers and cargo in metropolitan areas, which is designed to support a variety of on-board, ground-piloted and increasingly autonomous flight operations [1]. Some future concepts for on-demand mobility include fully autonomous vehicle operation using advanced sensing, perception, and navigation algorithms capable of replacing onboard pilot's functions. These type of operations in a dense and highly dynamic aerospace require the air vehicles be equipped with reliable sense and avoid (SAA) capability to maintain safe separation from terrain and other airborne objects[2, 3].

Traditionally, radio detection and ranging (radar) sensors have been used to detect obstacles such as terrains and air vehicles. Recently, they found widespread applications in autonomous driving and driver assistive systems as they have long ranges and are robust to atmospheric attenuation and lighting conditions. However, size, weight, power and cost (SWAP-C) limitations create challenges in reliably achieving desired obstacle (target) detection and estimation results for unmanned aircraft systems [4].

Radar sensors used for target tracking are conventionally modeled to provide measurements of the target's relative to the sensor range and angles, and in some cases also range rate, with uncertainties normally assumed to be zero-mean, Gaussian distributed, and uncorrelated [5]. In general, range and angle measurements may have different accuracy depending on the sensors configurations. For example, a phased array radar has more accurate range measurements than angle measurements, which can be inferred from the analysis of the estimation error covariance ellipsoid, which looks like a pancake normal to the range vector. In case of a continuous-wave radar, the situation is reversed, and the error covariance ellipsoid has a cigar-shape along the range vector [6]. As it was mentioned in Ref. [1], these latter type of radars may be suitable for small aircraft systems in terrain detection and dynamic obstacle tracking for safe and reliable


*ESOF40-Technical Advisor, KBR Wyle Services, Intelligent Systems Division, Mail Stop 269-1, email: vahram.stepanyan@nasa.gov
†Aerospace Research Engineer, KBR Wyle Services, Intelligent Systems Division, Mail Stop 269-1, email: thomas.lombaerts@nasa.gov
‡Aerospace Engineer, Aeronautics Systems Engineering Branch, email: chester.v.dolph@nasa.gov
§Aerospace Research Engineer, Intelligent Systems Division, Mail Stop 269-1, email: corey.a.ippolito@nasa.gov

AAM operations. From this perspective it is worth to take a second look at radar sensor's range measurement model. As far a the target motion is concerned, a good survey of more or less standard models can be found in Ref. [9], where the control input for target maneuvers is consider as a random process belonging to three main groups of White, Markov and Semi-Markov jump processes.

Usually, the tracking problem is considered in a mixed continuous-discrete time domain, where the target dynamics are in continuous-time and the measurements are in discrete-time, which is an optimal choice in many tracking and navigation applications. The target motion is commonly considers as a continuous time coordinate-uncoupled white-noise acceleration model for a point object [8], which is linear in states, while the measurements are nonlinear, hence the Extended Kalman Filter (EKF) framework is used for target tracking in many applications.

Alternatively, the measurements can be converted from spherical coordinates into Cartesian ones, thus making the new measurements linear in states, hence suitable for the standard Kalman filter application. However, there are several challenges in this approach, the critical ones being the conversion biases and computation of the converted measurement error covariance, because biased measurements violate the main assumption of the Kalman filter and the converted measurements covariance depends on the true states, which are unavailable. Several methods were reported in the literature to overcome these challenges, which include the unbiased converted measurement (UCM) [14], the modified unbiased converted measurement (MUCM) [15, 16], the unscented transform (UT)[17], best linear unbiased estimator (BLUE) [18], and de-correlated unbiased converted measurement (DUCM) [19]. It has been shown that, the performance of a converted measurement Kalman Filter (CMKF) is better than the mixed coordinate EKF, if the conversion is unbiased [20]. Ideally, besides being unbiased the conversion should also be consistent, provide minimum mean square error estimates and not suffer from estimation biases. In many cases, it is hard for a specific conversion method to satisfy all this requirements, and trade-off is made usually at expense of mean square errors.

This paper focuses on the improvement of target tracking accuracy taking into account the sensor's reading degradation as the relative range increases. The approach is based on the assumption that range measurement error depends on the actual range. Similar idea was used in Ref. [7] to derive estimation bounds in radar target tracking assuming that the range measurement error upper bound is proportional to the actual range itself. Specifically, we model the measurement error as a proportional to the actual range term plus a zero-mean, Gaussian distributed, and uncorrelated process. We present two approaches to tracking a target with constant velocity model. The first approach uses Extended Kalman Filter (EKF) framework to estimate target's state and the unknown proportionality coefficient with linearization of the observation model on the predicted states at each time step. The second one uses a measurement conversion method similar to DUCM presented in [10] to estimate the target's scaled by the unknown constant term states, which is shown to be unbiased. The converted error covariance matrix is approximated at each time step using the predicted states. This type of conversion results in linear state and observation models, hence the standard Kalman filter can be applied. The actual target states are computed by application of back scaling with the estimate of the unknown scale factor. We evaluate the approaches in desktop simulations using Matlab Simuink.

## II. Problem Formulation

We consider a target estimation/tracking problem in continuous-discrete time domain, that is, the target dynamics are in continuous-time and the measurements are in discrete-time with a time step $\delta t$, which is the optimal choice in many publications for tracking and navigation application (see for example [11–13] and references therein). Let the target motion be given by the following continuous time coordinate-uncoupled white-noise acceleration model in Cartesian coordinate system $\{x,\ y,\ z\}$

$$\begin{aligned} \ddot{x}(t) &= n_x(t) \\ \ddot{y}(t) &= n_y(t) \\ \ddot{z}(t) &= n_z(t)\,, \end{aligned} \tag{1}$$

where $n_x(t),\ n_y(t),\ n_z(t)$ are zero-mean, Gaussian distributed, and uncorrelated processes with variances $\sigma_x^2,\ \sigma_y^2,\ \sigma_z^2$. The observation model is given in $3D$ spherical coordinate system $\{r,\ \theta,\ \phi\}$ as

$$\begin{aligned} r_m(k) &= r(k) + br(k) + n_r(k) \\ \theta_m(k) &= \theta(k) + n_\theta(k) \\ \phi_m(k) &= \phi(k) + n_\phi(k)\,, \end{aligned} \tag{2}$$

where subscript $m$ indicates the measured value of the corresponding quantity, $f(r(k))$ represents a range dependent measurement error term, $n_r(t),\ n_\theta(k),\ n_\phi(k)$ are assumed to be zero-mean, Gaussian distributed, and uncorrelated processes with variances $\sigma_r^2,\ \sigma_\theta^2,\ \sigma_\phi^2$, and $b$ is assumed to be an unknown constant.

### A. Mixed Cartesian-Spherical Framework

In this case the target's motion is in Cartesian and the observation model is in spherical coordinates, as commonly used. We use Extended Kalman Filter (EKF) framework for the target tracking, with motion model disctretization and observation model linearization. To this end, we employ the dicretized 7th order motion model

$$\boldsymbol{s}(k) \quad = \quad \Phi(k-1)\boldsymbol{s}(k-1) + \Gamma(k-1)\boldsymbol{w}(k-1)\,, \tag{3}$$

where the vector $\boldsymbol{s}(k) = [x(k)\ \ \dot{x}(k)\ \ y(k)\ \ \dot{y}(k)\ \ z(k)\ \ \dot{z}(k)\ \ b(k)]^\top$ represents the target states and the unknown constant $b$, $\boldsymbol{w}(k) = [n_x(k)\ \ n_y(k)\ \ n_z(k)\ \ n_b(k)]^\top$ is the input noise vector, which also includes a zero-mean Gaussian white noise $n_b(k)$ with a variance $\sigma_b^2$ that drives evolution of the unknown term $b$,

$$\Phi(k) = \begin{bmatrix} 1 & \delta t & 0 & 0 & 0 & 0 & 0 \\ 0 & 1 & 0 & 0 & 0 & 0 & 0 \\ 0 & 0 & 1 & \delta t & 0 & 0 & 0 \\ 0 & 0 & 0 & 1 & 0 & 0 & 0 \\ 0 & 0 & 0 & 0 & 1 & \delta t & 0 \\ 0 & 0 & 0 & 0 & 0 & 1 & 0 \\ 0 & 0 & 0 & 0 & 0 & 0 & 1 \end{bmatrix},\ \Gamma(k) = \begin{bmatrix} \delta t^2/2 & 0 & 0 & 0 \\ \delta t & 0 & 0 & 0 \\ 0 & \delta t^2/2 & 0 & 0 \\ 0 & \delta t & 0 & 0 \\ 0 & 0 & \delta t^2/2 & 0 \\ 0 & 0 & \delta t & 0 \\ 0 & 0 & 0 & \delta t \end{bmatrix}$$

are the state transition and input matrices. The system of equations (3) and (2) is in a standard form for the EKF application, which we outline here for completeness:

1) predict the state and covariance estimate

$$\begin{aligned} \hat{\boldsymbol{s}}(k|k-1) &= \Phi(k)\hat{\boldsymbol{s}}(k-1|k-1) \\ P(k|k-1) &= \Phi(k)P(k|k-1)\Phi^\top(k) + \Gamma(k)Q(k)\Gamma^\top(k)\,, \end{aligned} \tag{4}$$

2) predict measurement estimates

$$\begin{aligned} \hat{r}(k|k-1) &= \sqrt{\hat{s}_1^2(k|k-1) + \hat{s}_3^2(k|k-1) + \hat{s}_5^2(k|k-1)} \\ \hat{\theta}(k|k-1) &= \arctan 2\left(\hat{s}_3(k|k-1), \hat{s}_1(k|k-1)\right) \\ \hat{\phi}(k|k-1) &= \arctan 2\left(\hat{s}_5(k|k-1), \sqrt{\hat{s}_1^2(k|k-1) + \hat{s}_3^2(k|k-1)}\right) \\ \hat{\boldsymbol{u}}(k|k-1) &= \left[(1+\hat{b}(k|k-1))\hat{r}(k|k-1)\ \ \hat{\theta}(k|k-1)\ \ \hat{\phi}(k|k-1)\right]^\top\,, \end{aligned} \tag{5}$$

3) compute Jacobean of the observation model on the predicted states $\hat{\boldsymbol{s}}(k|k-1)$

$$H(k) = \begin{bmatrix} (1+\hat{b})\cos(\hat{\phi})\cos(\hat{\theta}) & 0 & (1+\hat{b})\cos(\hat{\phi})\sin(\theta) & 0 & (1+\hat{b})\sin(\hat{\phi}) & 0 & \hat{r} \\ -\frac{\sin(\hat{\theta})}{\hat{r}\cos(\hat{\phi})} & 0 & \frac{\cos(\hat{\theta})}{\hat{r}\cos(\hat{\phi})} & 0 & 0 & 0 & 0 \\ -\frac{\sin(\hat{\phi})\cos(\hat{\theta})}{\hat{r}} & 0 & -\frac{\sin(\hat{\phi})\sin(\hat{\theta})}{\hat{r}} & 0 & \frac{\cos(\hat{\phi})}{\hat{r}} & 0 & 0 \end{bmatrix},$$

where time dependence is omitted for the notation convenience,

4) compute Kalman Gain

$$K(k) \quad = \quad P(k|k-1)H(k)^\top\left[H(k)P(k|k-1)H(k)^\top + R(k)\right]^{-1}\,, \tag{6}$$

5) update estimates

$$\begin{aligned} \hat{\boldsymbol{s}}(k|k) &= \hat{\boldsymbol{s}}(k|k-1) + K(k)\left[\boldsymbol{u}(k) - \hat{\boldsymbol{u}}(k)\right] \\ P(k|k) &= \left[\mathbb{I}_{7\times7} - K(k)H(k)\right]P(k|k-1)\,, \end{aligned} \tag{7}$$

where we denote $\boldsymbol{u}(k) = [r_m(k)\ \ \theta_m(k)\ \ \phi_m(k)]^\top$.

### B. Cartesian Framework With Measurement Conversion

In this case, the measurements are transformed from the spherical coordinate system into the Cartesian via a nonlinear transformation, which results in linear dependency of converted measurements on the states, hence the linear estimation is applicable with a guaranteed convergence and quantifiable error bounds. However, there are challenges related to the conversion biases, since a fundamental assumption in the Kalman filter is that the measurement errors are unbiased, and related to the converted measurement error covariance computation, since it depends on the unavailable true states.

Here we follow the steps of DUCM to convert the range depended measurements in (2) to Cartesian coordinates and express new measurements as

$$\begin{aligned}\bar{x}_m &= \exp\left(\frac{\sigma_\theta^2}{2}\right)\exp\left(\frac{\sigma_\phi^2}{2}\right) r_m \cos(\theta_m)\cos(\phi_m) \\ \bar{y}_m &= \exp\left(\frac{\sigma_\theta^2}{2}\right)\exp\left(\frac{\sigma_\phi^2}{2}\right) r_m \sin(\theta_m)\cos(\phi_m) \\ \bar{z}_m &= \exp\left(\frac{\sigma_\phi^2}{2}\right) r_m \sin(\phi_m)\,. \end{aligned} \tag{8}$$

It is clear from the representation $r_m = r(1+b)r + n_r$ that the converted measurements $\bar{x}_m,\ \bar{y}_m,\ \bar{z}_m$ represent not the target's true but scaled Cartesian coordinates $\bar{x} = (1+b)x,\ \bar{y} = (1+b)y,\ \bar{z} = (1+b)z$. Therefore, the application of standard Kalman filter to the system (3) with measurements (8) computes the estimates of the scaled states $\hat{\bar{x}}(k) = (1+\hat{b}(k))\hat{x}(k),\ \hat{\bar{y}}(k) = (1+\hat{b}(k))\hat{y}(k),\ \hat{\bar{z}}(k) = (1+\hat{b}(k))\hat{z}(k)$. That is the estimates of target's true position can be computed by Kalman filter output scaling as

$$\hat{x}(k|k) = \frac{\hat{\bar{s}}_1(k|k)}{1+\hat{\bar{s}}_7(k|k)}, \quad \hat{y}(k|k) = \frac{\hat{\bar{s}}_3(k|k)}{1+\hat{\bar{s}}_7(k|k)}, \quad \hat{z}(k|k) = \frac{\hat{\bar{s}}_5(k|k)}{1+\hat{\bar{s}}_7(k|k)}\,, \tag{9}$$

where $\hat{\bar{\mathbf{s}}}(k|k) = \left[\hat{\bar{s}}_1(k|k) \ldots \hat{\bar{s}}_7(k|k)\right]^\top$ is the filter output at time $k$.

To make sure that the conversion (8) is unbiased, we show that the expected values satisfy equations of $E\left\{\bar{x}_m\right\} = \bar{x}$, $E\left\{\bar{y}_m\right\} = \bar{y}$, and $E\left\{\bar{z}_m\right\} = \bar{z}$. Since the range, azimuth and elevation measurement noise terms are uncorrelated, zero-mean Gaussian, we can write for $\bar{x}_m$

$$\begin{aligned} E\left\{\bar{x}_m\right\} &= \exp\left(\frac{\sigma_\theta^2}{2}\right)\exp\left(\frac{\sigma_\phi^2}{2}\right) E\left\{(r+br+n_r)\cos(\theta+n_\theta)\cos(\phi+n_\phi)\right\} && (10)\\ &= \exp\left(\frac{\sigma_\theta^2}{2}\right)\exp\left(\frac{\sigma_\phi^2}{2}\right) E\left\{(r+br+n_r)\right\} E\left\{\cos(\theta+n_\theta)\right\} E\left\{\cos(\phi+n_\phi)\right\} \\ &= (1+b)r\cos(\theta)\cos(\phi) = \bar{x}\,. && (11)\end{aligned}$$

The remaining equations are shown similarly.

We notice that the process noise variances are being scaled as well, but these are design parameters. On the other hand, the converted measurements error covariance matrix $R^c$ is sensor depended and needs to be estimated using representation (8). For the convenience of derivations, it is computed in terms of spherical coordinates using predicted states for each time step.

Let at radar scan $k-1$ the $k-th$ predictions of the true values $r(k),\ \theta(k),\ \phi(k)$ be

$$\hat{r}(k|k-1) = r(k) + v_r(k), \quad \hat{\theta}(k|k-1) = \theta(k) + v_\theta(k), \quad \hat{\phi}(k|k-1) = \phi(k) + v_\phi(k)\,, \tag{12}$$

where $\hat{r}(k|k-1),\ \hat{\theta}(k|k-1),\ \hat{\phi}(k|k-1)$ are the predictions and $v_r(k),\ v_\theta(k),\ v_\phi(k)$ are corresponding errors, which are assumed to be zero mean Gaussian with standard deviations $\sigma_{v_r},\ \sigma_{v_\theta},\ \sigma_{v_\phi}$. These predictions are expressed trough state $\hat{\bar{\mathbf{s}}}(k|k-1)$ as

$$
\begin{aligned}
\hat{r}(k|k-1) &= \frac{1}{1+\hat{\hat{s}}_7(k|k-1)}\sqrt{\hat{\hat{s}}_1^2(k|k-1)+\hat{\hat{s}}_3^2(k|k-1)+\hat{\hat{s}}_5^2(k|k-1)} \\
\hat{\theta}(k|k-1) &= \arctan 2\left(\hat{\hat{s}}_3(k|k-1), \hat{\hat{s}}_1(k|k-1)\right) \\
\hat{\phi}(k|k-1) &= \arctan 2\left(\hat{\hat{s}}_5(k|k-1), \sqrt{\hat{\hat{s}}_1^2(k|k-1)+\hat{\hat{s}}_3^2(k|k-1)}\right) \qquad (13)
\end{aligned}
$$

Let the prediction of the covariance matrix at time $k$ from the standard Kalman filter be $\bar{P}(k|k-1)$. Then at time $k$ given the scan $k-1$, the range prediction variance can be expressed as (time notation $(k|k-1)$ is omitted for simplicity)

$$
\sigma_{v_r}^2 = [\nabla\hat{r}]\,\bar{P}\,[\nabla\hat{r}]^\top , \qquad (14)
$$

where $\nabla\hat{r}$ is computed from (13) as

$$
\nabla\hat{r} = \left[\frac{\hat{\hat{s}}_1}{[1+\hat{\hat{s}}_7]^2\hat{r}} \;\; 0 \;\; \frac{\hat{\hat{s}}_3}{[1+\hat{\hat{s}}_7]^2\hat{r}} \;\; 0 \;\; \frac{\hat{\hat{s}}_5}{[1+\hat{\hat{s}}_7]^2\hat{r}} \;\; 0 \;\; -\frac{\hat{r}}{1+\hat{\hat{s}}_7}\right] . \qquad (15)
$$

The gradients of azimuth and elevation angles predictions with respect to state estimates are computed similarly

$$
\begin{aligned}
\nabla\hat{\theta} &= \frac{1}{[1+\hat{\hat{s}}_7]^2\hat{r}^2}\left[-\hat{\hat{s}}_3 \;\; 0 \;\; \hat{\hat{s}}_1 \;\; 0 \;\; 0 \;\; 0 \;\; 0\right] \\
\nabla\hat{\phi} &= \frac{1}{[1+\hat{\hat{s}}_7]^2\hat{r}^2\sqrt{\hat{\hat{s}}_1^2+\hat{\hat{s}}_3^2}}\left[-\hat{\hat{s}}_1\hat{\hat{s}}_5 \;\; 0 \;\; -\hat{\hat{s}}_3\hat{\hat{s}}_5 \;\; 0 \;\; \hat{\hat{s}}_1^2+\hat{\hat{s}}_3^2 \;\; 0 \;\; 0\right] , \qquad (16)
\end{aligned}
$$

and are used to compute the prediction variances as

$$
\sigma_{v_\theta}^2 = \left[\nabla\hat{\theta}\right]\bar{P}\left[\nabla\hat{\theta}\right]^\top, \quad \sigma_{v_\phi}^2 = \left[\nabla\hat{\phi}\right]\bar{P}\left[\nabla\hat{\phi}\right]^\top . \qquad (17)
$$

Now we are ready compute the converted measurements error covariance. For the $R_{11}^c$ we obtain

$$
\begin{aligned}
R_{11}^c &= E\left\{\left[\hat{r}\cos(\theta)\cos(\phi) - \exp\left(\frac{\sigma_\theta^2}{2}\right)\exp\left(\frac{\sigma_\phi^2}{2}\right) r_m\cos(\theta_m)\cos(\phi_m)\right]^2\right\} \qquad (18) \\
&= E\left\{\left[(\hat{r}-v_r)\cos(\hat{\theta}-v_\theta)\cos(\hat{\phi}-v_\phi) - \exp\left(\frac{\sigma_\theta^2}{2}\right)\exp\left(\frac{\sigma_\phi^2}{2}\right)\right.\right. \\
&\cdot \left.\left.(1+\hat{\hat{s}}_7-n_b)((\hat{r}-v_r)+n_r)\cos(\hat{\theta}-v_\theta+n_\theta)\cos(\hat{\phi}-v_\phi+n_\phi)\right]^2\right\} \\
&= \frac{1}{4}\left(\left(\left(1+\hat{\hat{s}}_7\right)^2+\sigma_b^2\right)\left(\hat{r}^2+\sigma_{v_r}^2\right)+\sigma_r^2\right)\left[1+\cos(2\hat{\theta})\exp\left(-2\sigma_{v_\theta}^2\right)\exp\left(-2\sigma_\theta^2\right)\right] \\
&\cdot \exp\left(\sigma_\theta^2\right)\left[1+\cos(2\hat{\phi})\exp\left(-2\sigma_{v_\phi}^2\right)\exp\left(-2\sigma_\phi^2\right)\right]\exp\left(\sigma_\phi^2\right) \\
&- \left(\frac{1}{4}+\hat{\hat{s}}_7\right)\left(\hat{r}^2+\sigma_{v_r}^2\right)\left[1+\cos(2\hat{\theta})\exp\left(-2\sigma_{v_\theta}^2\right)\right]\left[1+\cos(2\hat{\phi})\exp\left(-2\sigma_{v_\phi}^2\right)\right] .
\end{aligned}
$$

The remaining terms are presented bellow

$$
\begin{aligned}
R_{22}^c &= \frac{1}{4}\left(\left(\left(1+\hat{\hat{s}}_7\right)^2+\sigma_b^2\right)\left(\hat{r}^2+\sigma_{v_r}^2\right)+\sigma_r^2\right)\left[1-\cos(2\hat{\theta})\exp\left(-2\sigma_{v_\theta}^2\right)\exp\left(-2\sigma_\theta^2\right)\right] \qquad (19) \\
&\cdot \exp\left(\sigma_\theta^2\right)\left[1+\cos(2\hat{\phi})\exp\left(-2\sigma_{v_\phi}^2\right)\exp\left(-2\sigma_\phi^2\right)\right]\exp\left(\sigma_\phi^2\right) \\
&- \left(\frac{1}{2}+\hat{\hat{s}}_7\right)\left(\hat{r}^2+\sigma_{v_r}^2\right)\left[1-\cos(2\hat{\theta})\exp\left(-2\sigma_{v_\theta}^2\right)\right]\left[1+\cos(2\hat{\phi})\exp\left(-2\sigma_{v_\phi}^2\right)\right]
\end{aligned}
$$

$$
\begin{aligned}
R^c_{33} &= \frac{1}{2}\left(\left(\left(1+\hat{\bar{s}}_7\right)^2+\sigma_b^2\right)\left(\hat{r}^2+\sigma_{v_r}^2\right)+\sigma_r^2\right)\left[1-\cos(2\hat{\phi})\exp\left(-2\sigma_{v_\phi}^2\right)\exp\left(-2\sigma_\phi^2\right)\right] \\
&\cdot \exp\left(\sigma_\phi^2\right)-\left(\frac{1}{2}+\hat{\bar{s}}_7\right)\left(\hat{r}^2+\sigma_{v_r}^2\right)\left[1-\cos(2\hat{\phi})\exp\left(-2\sigma_{v_\phi}^2\right)\right]
\end{aligned} \tag{20}
$$

$$
\begin{aligned}
R^c_{12} &= \frac{1}{4}\left(\left(\left(1+\hat{\bar{s}}_7\right)^2+\sigma_b^2\right)\left(\hat{r}^2+\sigma_{v_r}^2\right)+\sigma_r^2\right)\left[\sin(2\hat{\theta})\exp\left(-2\sigma_{v_\theta}^2\right)\exp\left(-2\sigma_\theta^2\right)\right] \\
&\cdot \exp\left(\sigma_\theta^2\right)\left[1+\cos(2\hat{\phi})\exp\left(-2\sigma_{v_\phi}^2\right)\exp\left(-2\sigma_\phi^2\right)\right]\exp\left(\sigma_\phi^2\right) \\
&- \left(\frac{1}{2}+\hat{\bar{s}}_7\right)\left(\hat{r}^2+\sigma_{v_r}^2\right)\left[\sin(2\hat{\theta})\exp\left(-2\sigma_{v_\theta}^2\right)\right]\left[1+\cos(2\hat{\phi})\exp\left(-2\sigma_{v_\phi}^2\right)\right]
\end{aligned} \tag{21}
$$

$$
\begin{aligned}
R^c_{13} &= \frac{1}{2}\left(\left(\left(1+\hat{\bar{s}}_7\right)^2+\sigma_b^2\right)\left(\hat{r}^2+\sigma_{v_r}^2\right)+\sigma_r^2\right)\cos(\hat{\theta})\exp\left(-\frac{\sigma_\theta^2}{2}\right)\left[\sin(2\hat{\phi})\exp\left(-2\sigma_{v_\phi}^2\right)\exp\left(-2\sigma_\phi^2\right)\right] \\
&\cdot \exp\left(\sigma_\phi^2\right)-\left(\frac{1}{2}+\hat{\bar{s}}_7\right)\left(\hat{r}^2+\sigma_{v_r}^2\right)\cos(\hat{\theta})\exp\left(-\frac{\sigma_\theta^2}{2}\right)\left[\sin(2\hat{\phi})\exp\left(-2\sigma_{v_\phi}^2\right)\right]
\end{aligned} \tag{22}
$$

$$
\begin{aligned}
R^c_{23} &= \frac{1}{2}\left(\left(\left(1+\hat{\bar{s}}_7\right)^2+\sigma_b^2\right)\left(\hat{r}^2+\sigma_{v_r}^2\right)+\sigma_r^2\right)\sin(\hat{\theta})\exp\left(-\frac{\sigma_\theta^2}{2}\right)\left[\sin(2\hat{\phi})\exp\left(-2\sigma_{v_\phi}^2\right)\exp\left(-2\sigma_\phi^2\right)\right] \\
&\cdot \exp\left(\sigma_\phi^2\right)-\left(\frac{1}{2}+\hat{\bar{s}}_7\right)\left(\hat{r}^2+\sigma_{v_r}^2\right)\sin(\hat{\theta})\exp\left(-\frac{\sigma_\theta^2}{2}\right)\left[\sin(2\hat{\phi})\exp\left(-2\sigma_{v_\phi}^2\right)\right].
\end{aligned} \tag{23}
$$

The estimation process follows the following steps:

1) predict the state and covariance estimate

$$
\begin{aligned}
\hat{\bar{\boldsymbol{s}}}(k|k-1) &= \Phi(k)\hat{\bar{\boldsymbol{s}}}(k-1|k-1) \\
\bar{P}(k|k-1) &= \Phi(k)\bar{P}(k|k-1)\Phi^\top(k)+\Gamma(k)Q(k)\Gamma^\top(k),
\end{aligned} \tag{24}
$$

2) compute residual as predict measurement estimates

$$
\tilde{\bar{\boldsymbol{u}}}(k) = \bar{\boldsymbol{u}}_m(k)-C\hat{\bar{\boldsymbol{s}}}(k|k-1), \tag{25}
$$

where $\bar{\boldsymbol{u}}_m(k)=[\bar{x}_m(k)\ \ \bar{y}_m(k)\ \ \bar{z}_m(k)]^\top$, $\bar{x}_m(k),\ \bar{y}_m(k),\ \bar{z}_m(k)$ are given by (8), and matrix $C$ has the form

$$
C=\begin{bmatrix} 1 & 0 & 0 & 0 & 0 & 0 & 0 \\ 0 & 0 & 1 & 0 & 0 & 0 & 0 \\ 0 & 0 & 0 & 0 & 1 & 0 & 0 \end{bmatrix},
$$

3) compute converted measurement covariance $R^c(k)$ according to (18)-(23)

4) compute Kalman Gain

$$
\bar{K}(k) = \bar{P}(k|k-1)C^\top\left[C\bar{P}(k|k-1)C^\top+R^c(k)\right]^{-1}, \tag{26}
$$

5) update estimates

$$
\begin{aligned}
\hat{\bar{\boldsymbol{s}}}(k|k) &= \hat{\bar{\boldsymbol{s}}}(k|k-1)+\bar{K}(k)\tilde{\bar{\boldsymbol{u}}}(k) \\
\bar{P}(k|k) &= \left[\mathbb{I}_{7\times 7}-\bar{K}(k)C\right]\bar{P}(k|k-1).
\end{aligned} \tag{27}
$$

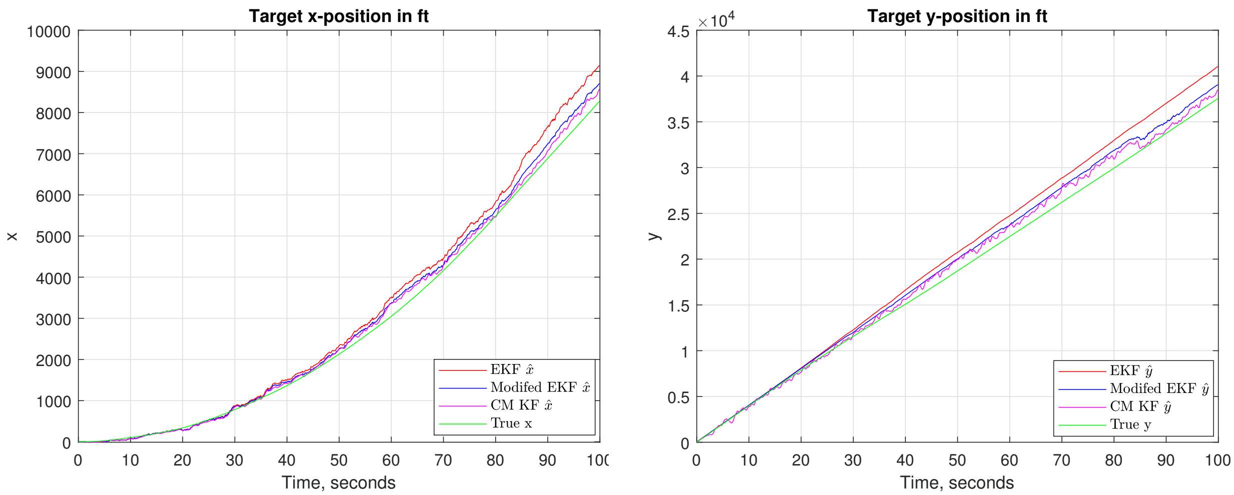


**(a) x-coordinate estimates and true value (green)** **(b) y-coordinate estimates and true value (green)**

**Fig. 1 Target coordinates**

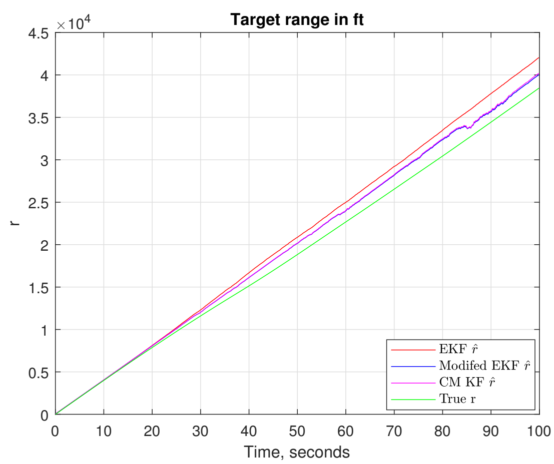


**Fig. 2 Target range.**

# III. Simulation Results

We evaluate the proposed sensor model in Matlab simulations for a target $2D$ motion. We compare three approached: EKF with conventional sensor model in mixed Cartesian-Spherical framework, EKF with proposed sensor model (modified EKF) in mixed Cartesian-Spherical framework, and standard KF in Cartesian framework with measurement conversion (CM KF). Let the target moves with speed of $400 ft/sec$ in $y$-direction from the initial position of $(0,\ 0) ft$ with $\sigma_x^2 = \sigma_y^2 = 0.005$. The measurement noise standard deviation was set to $\sigma_r = 300$, $\sigma_\theta = 0.001$ and the unknown constant is $b = 0.1$ with $\sigma_b^2 = 0.005$.

Fig. 1 shows target's $(x,\ y)$-position estimation results, where green lines represent the true positions. It can be observed that the performance of EKF with conventional sensor model is the worst, which was expected since it does not have any information on range measurement error model. The performance of the other two filters are somewhat close albeit CM KF produces noisier results, which were smoothed by a Gaussian filter with a window of width 9 prior to plotting. The corresponding range estimates are displayed in Fig.2, with similar performances.

Fig. 3 displays target's velocity estimates along with the true values (green lines). It can be observed that the x-velocity estimates are initially almost identical for all estimation methods, but EKF performance gets worse at the end of simulation interval. In y-direction the CM KF performance is initially the worst, but gets improved as the simulation

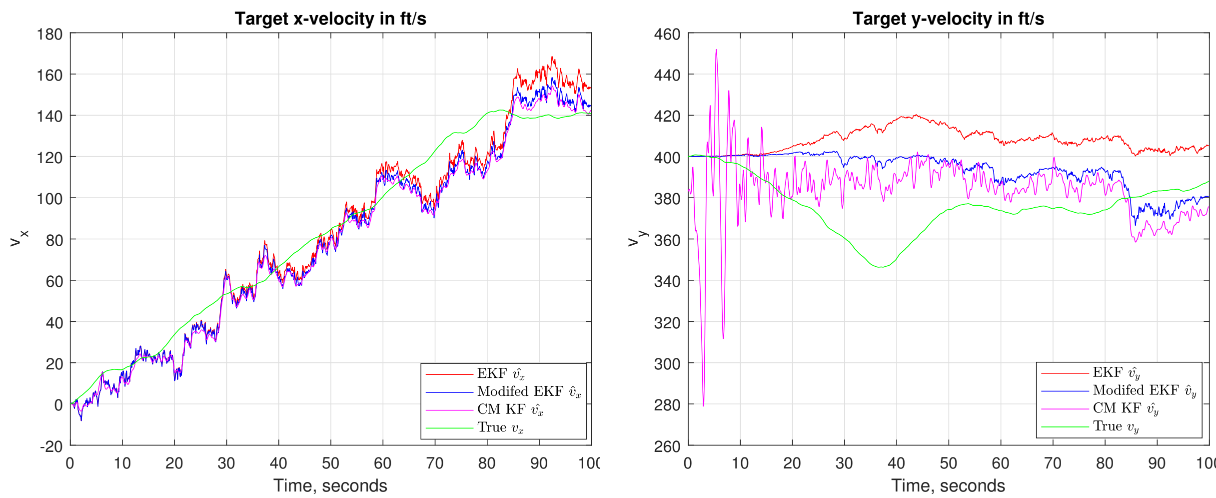


**(a) x-velocity estimates and true value (green)** **(b) y-velocity estimates and true value (green)**

**Fig. 3 Target velocities**

progresses. This can be explained by the comparably large initialization error.

For the clarity, we also plotted the estimation errors in Fig.4 and Fig.5. It can be observed that the errors are almost identical at the beginning of simulation, but the EKF error grows large as the simulation progresses, which was expected. The errors of other two methods are comparable, but CM KF produces more oscillatory error. This is attributed to division of CM KF output by $1 + \hat{b}(k)$.

Fig. 6 displays the estimation results of unknown constant $b$. Initial large estimation errors of in modified EKF are decreased as the simulation progresses, but there is no convergence to the true value of 0.1

# IV. Conclusion

We have presented a framework to improve the target tracking accuracy taking into account the sensor's reading degradation as the relative range increases, assuming that the measurement error is represented as a proportional to the actual range term plus a zero-mean Gaussian noise. First, we used Extended Kalman Filter (EKF) to estimate target's state and the unknown proportionality coefficient with linearization of the observation model on the predicted state at each time step. Then, we used a measurement conversion method to estimate the target's scaled by the unknown constant term state, which is shown to be unbiased. This type of conversion results in linear state and observation models with unbiased measurements, hence the standard Kalman filter can be applied. The actual target state is computed by application of back scaling with the estimate of unknown scale factor. We have evaluated the approaches in desktop simulations, and obtained comparable results.

The future research will include proposed sensor model validation with actual flight test data Monte-Carlo type simulation analysis.

# Acknowledgment

This work was performed under the NASA Aeronautics Research Mission Directorate (ARMD), Transformative Tools and Technologies (TTT) Project's Autonomous Systems activity.

# References

[1] K. H. Shish, N. B. Cramer, G. Gorospe, T, Lombaerts, V. Stepanyan and K. Kannan. Survey of Capabilities and Gaps in External Perception Sensors for Autonomous Urban Air Mobility Applications, *I*n Proc. of the AIAA Scitech 2021 Forum, 11–15 & 19–21 January 2021, Virtual Event, https://doi.org/10.2514/6.2021-1114.

[2] G. Fasano, D. Accado, A. Moccia, and D. Moroney. Sense and Avoid for Unmanned Aircraft Systems, *I*EEE Aerospace and Electronic Systems Magazine, Vol. 31, No. 11, 2016, pp. 82–110.

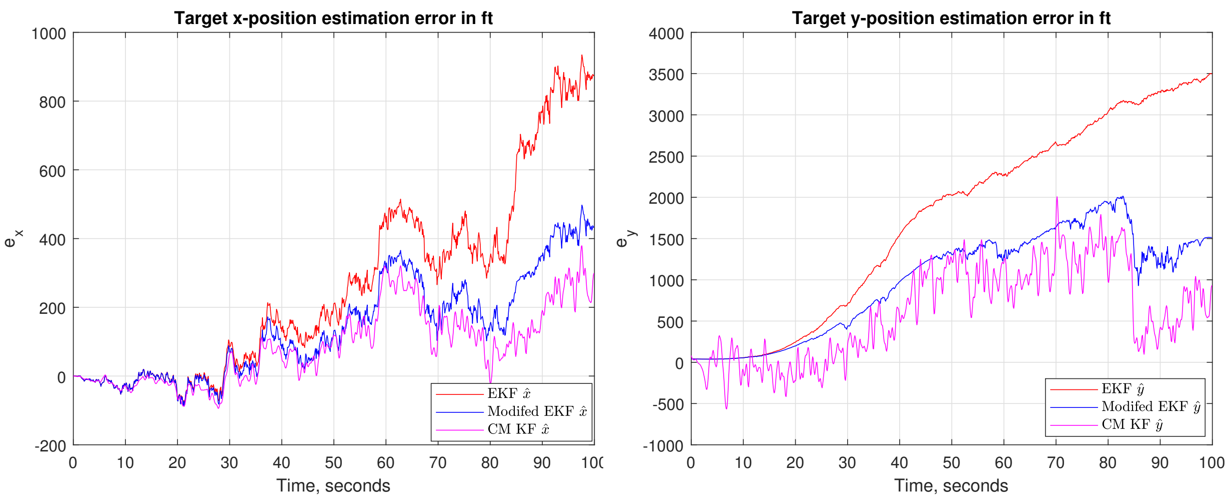


**(a) x-coordinate estimation errors** **(b) y-coordinate estimation errors**

**Fig. 4 Target coordinates estimation errors**

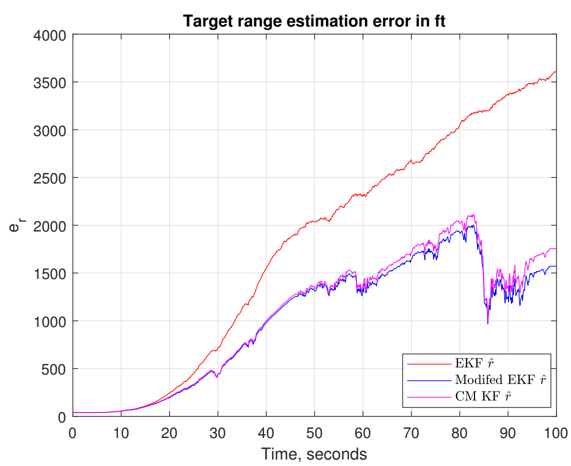


**Fig. 5 Target range estimation errors.**

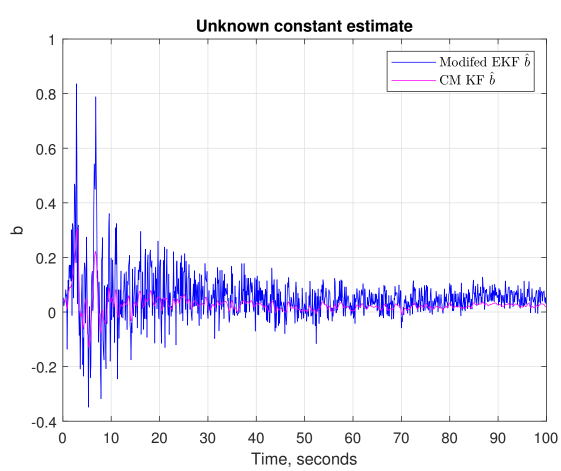


**Fig. 6 Unknown constant estimates.**

[3] A. Straubinger, R. Rothfeld, M. Shamiyeh, K.-D. Büchter, J. Kaiser, and K. O. Plötnera. An overview of current research and developments in urban air mobility – Setting the scene for UAM introduction, Journal of Air Transport Management, Volume 87, August 2020, https://doi.org/10.1016/j.jairtraman.2020.101852.

[4] C. Serres and M. Wu. Low C-SWaP Detect and Avoid: Defining Well Clear, MIT Lincoln Labs Air Traffic Control Workshop, Washington DC, November 2019, URL https://ntrs.nasa.gov/archive/nasa/casi.ntrs.nasa.gov/20200000623.pdf.

[5] X. R. Li and V. P. Jilkov. A Survey of Maneuvering Target Tracking—Part III: Measurement Models. *In Proc. of SPIE, Volume 4473, Signal and Data Processing of Small Targets 2001*, page 423-446, doi: 10.1117/12.492752

[6] F. E. Daum and R. J. Fitzgerald. Decoupled Kalman Filters for Phased Array Radar Tracking. *IEEE Transactions on Automatic Control, Vol. Ac-28, No. 3, March 1983* , page 269-283, doi: 10.1117/12.492752

[7] A. N. Bishop, P. N. Pathirana, and A. V. Savkin. Radar Target Tracking via Robust Linear Filtering. *IEEE Signal Processing Letters, Vol. 14, No. 12, December 2007*, page 1028-1031, doi: 10.1109/LSP.2007.907993

[8] Y. Bar-Shalom, X. R. Li, and T. Kirubarajan. Estimation with Applications to Tracking and Navigation: Theory, Algorithms, and Software. *New York: Wiley, 2001*

[9] X. R. Li and V. P. Jilkov. Survey of Maneuvering Target Tracking. Part I: Dynamic Models. *IEEE Transactions on Aerospace and Electronic Systems, Vol. 50, No. 12, April 2014*, page 1431-1444

[10] S. Bordonaro, P. Willett, and Y. Bar-Shalom. Decorrelated, Unbiased Converted Measurement Kalman Filter. *IEEE Transactions on Aerospace and Electronic Systems, Vol. 39, No. 4, October 2003*, page 1333-1364

[11] I. Arasaratnam, S. Haykin, and T. R. Hurd. Cubature Kalman filtering for continuous-discrete systems: theory and simulations. *IEEE Transactions on Signal Processing, Vol. 58, No. 10, 2010*, page 4977–4993

[12] D. Crouse. Basic tracking using nonlinear continuous-time dynamic models. *IEEE Aerospace and Electronic Systems Magazine, Vol. 30, No. 2, 2015*, page 4-41

[13] G. Y . Kulikov and M. V. Kulikova. The accurate continuous-discrete extended kalman filter for radar tracking. *IEEE Transactions on Signal Processing, Vol. 64, No. 4, 2016*, page 948–958

[14] L. Mo, X. Song, Y. Zhou, Z. Sun, and Y. Bar-Shalom. Unbiased converted measurements for tracking. *IEEE Transactions on Aerospace and Electronic Systems, Vol. 34, No. 3, 1998*, page 1023–1027

[15] M. D. Miller and O. E. Drummond. Comparison of methodologies for miti-gating coordinate transformation bias in target tracking. *Proceedings of SPIE Conference on Signal and Data Processing of Small Targets, Vol. 4048, 2000*, page 414–427

[16] Z. Duan, C. Han, and X. R. Li. Comments on unbiased converted measurements for tracking. *IEEE Transactions on Aerospace and Electronic Systems, Vol. 40, No. 4, 2004*, page 1374–1377

[17] S. Julier and J. Uhlmann. A consistent, debiased method for converting between polar and Cartesian coordinate systems. *Proceedings of SPIE Conference on AeroSense: Acquisition, Tracking and Pointing XI (Orlando, FL, USA), Vol. 34, Oct. 1997*, page 110-121

[18] Z. Zhao, X. R. Li, V. P. Jilkov, and Y. Zhu. Optimal linear unbiased filtering with polar measurements for target tracking. *Proceedings of the Fifth International Conference on Information Fusion, Vol. 2, 2002*, page 1527-1534

[19] S. Bordonaro, P. Willett, and Y. Bar-Shalom. Tracking with converted position and Doppler measurements. *Proceedings of SPIE Conference on Signal and Data Processing of Small Targets, Vol. 8137, 2011*,

[20] D. Lerro and Y. Bar-Shalom. Tracking with debiased consistent converted measurements versus EKF. *IEEE Transactions on Aerospace and Electronic Systems, Vol. 29, No. 3, 1993*, page 1015–1022